ICONS-2014: International Conference on Structural Integrity, February 4-7, 2014, Kalpakkam, TN, India.

Realisation of Shear Flow at Crucial Spar Splice Joints of Composite Wing in Idealised Wing Test Box

Polagnagu James[1a], Kotresh Gaddikeri [2], Byji Varughese [2], M. Subba Rao[3]

[1] Sr. Scientist, [2] Principal Scientist, [3] Former Head of Division

Advanced Composites Division
CSIR-National Aerospace Laboratories
Kodihalli, Bangalore-560017, India
[a] james@nal.res.in

ABSTRACT: *CSIR -National Aerospace Laboratories (CSIR-NAL) has developed a patented processing technique called "Vacuum Enabled Resin Infusion Technology (VERITy" for the manufacturing of composite wing for its transport aircraft programme. The building block approach was adopted during the design stage of the composite wing to understand the structural response in increasingly complex structural levels. In the subcomponent level, a wing test box was designed, fabricated and was subjected to structural static testing for critical loads of the wing. The wing test box which was idealized into a rectangular box included the most critical joints such as top & bottom skin splice joints and front & rear spar splice joints. The stacking sequence and thickness of laminates used in the respective positions in wing test box replicated the wing structure. The challenge was to maintain the shear flow despite differences in the geometry of wing and test box without compromising on the magnitude of shear force at the critical spar splice joint. This paper discusses the methodology adopted for transforming shear flow from wing structure on to the idealized wing test box.*

Keywords: *Wing test box, transport aircraft, VERITy process, Shear flow, Skin and spar splice*

Nomenclature

A	*Area enclosed by the center line of closed box*
b_1, t_1	*Width and thickness of top skin*
b_2, t_2	*Height and thickness of front spar*
b_3, t_3	*Width and thickness of bottom skin*
b_4, t_4	*Height and thickness of rear spar*
e_x	*Position of shear center from front spar reference*
$F_{(1-2)}$	*Shear force acting in top skin*
$F_{(2-3)}$	*Shear force acting in front spar*
$F_{(3-4)}$	*Shear force acting in bottom skin*
$F_{(4-1)}$	*Shear force acting in rear spar*
G	*Shear modulus of a given member*
H_f	*Height of front spar of wing*
H_i	*Height of idealized wing structure*
H_w	*Height of wing test box*
I_{ij}	*Moment of inertia about i^{th}, j^{th} axis*
q_n^i,	*Shear flow value in idealized section at a point*
q_n^w	*Shear flow value in actual wing section at a point*
q_s	*Total shear flow in closed box structure*
q_b	*Base shear flow of an open section*
$q_{s,o}$	*Shear flow due to applied torque*
S_x	*Applied shear force along global x-axis*
S_y	*Applied shear force along global y- axis*

1. Introduction

In the current airframes, the use of carbon fibre composites (CFC) components has moved from secondary level to primary structural component level in both military and transport aircrafts. In the Indian scenario, the usage of composites in aircraft programs like light combat aircraft (LCA), SARAS, HANSA, Advanced Light Helicopter (ALH) etc. is substantial. Majority of these structures have been fabricated using prepregs and autoclave moulding technology. Prepregs have certain limitations, like the need of an autoclave, energy intensive, storage at -18°C, limited shelf life and outlife. Industry has adopted liquid composite moulding technologies to reduce the cost while maintaining nearly similar performance levels as compared to prepreg and autoclave moulding technology. Several variants of VARTM (Vacuum Assisted Resin Transfer Moulding) have been attempted by various researchers. In these lines, CSIR-NAL has developed a patented process called VERITy (Vacuum Enhanced Resin Infusion Technology) for developing large sized cocured

components. This is a hybrid of VARTM and autoclave technology. The wing structure of transport aircraft is proposed to be manufactured using VERITy process using carbon epoxy composites.

Considering the importance of the structure and the newness of the process, a building block approach was used in the design of wing. As a part of this approach, a wing test box was designed, fabricated and tested. The portion of wing test box was chosen so as to include the most critical splice joints in the composite wing. The objective was to have similar layups and features in the wing test box as compared to the wing in the chosen region. The major challenge in design emerged from the geometry wherein wing was of aerofoil contour as against the wing test box which was of constant height. The change in geometrical parameters does not allow splice plates to realise the critical stress flow when subjected to same loading systems that is acting on wing structure. A new system of loading was worked out so as to simulate the critical shear stress flow with the changed geometrical parameters. Furthermore, the mapping of shear flow from wing to test box was done so as to induce the criticality associated with that shear force at the spar splice joint. This paper discusses the methodology of shear flow simulation and the subsequent formulation of loading system for the wing test box whose size, span and geometry are different from that of wing.

2. Geometry of wing

The wing structure is a two spar construction with 23 inters spar rib stations each on LH / RH side of the wing. The wing is divided into three segments viz., two outboard segments and one centre segment. Both top and bottom skins are spliced between at #6 whereas front and

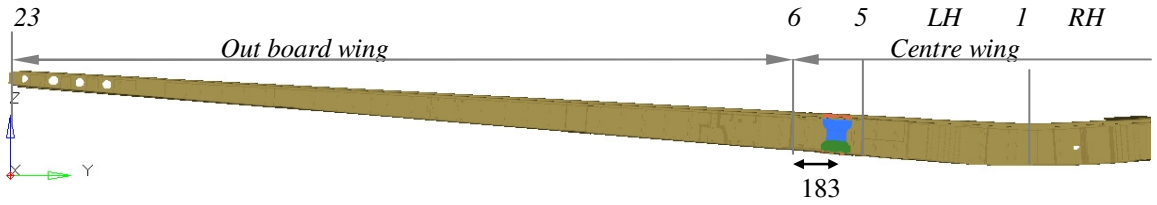

Fig. 1 Rear view of LH wing of composite wing structure showing position of spar splice joint

rear spars are spliced between station 5 and 6 with an offset of 183 mm towards inboard from skin splice joint. Bottom skins of each segment are cocured with both spars and interspar ribs. The location of spar splice is shown in Fig.1. At the feature level, both the skin and spar splice test specimens were tested separately [1, 2]. These test specimens represented the fastening systems, pattern of fasteners and also induced the critical stress flow in the composite splice plates. The spar splice and skin splice joints individually withstood design ultimate loads.

2.1. Splice plates

The shape of splice plates of front and rear spars are shown in Fig. 2 and Fig.3 respectively. Typical arrangement of fasteners connecting splice plates to the web and flange of spars are explained by the authors in design of spar splice joint in composite wing [1]. The stacking sequence and size of these splice plates were arrived at based on the critical design load acting on wing structure.

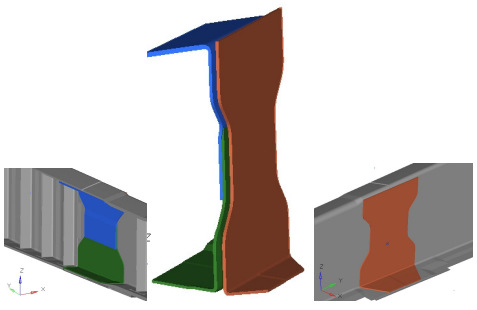

Fig. 2 Front spar splice plates and front and rear views

3. Fabrication method

The fabrication of composites components for wing test box is through the same fabrication process which is ultimately going to be used for making the parts of wing of multirole transport aircraft. The qualification of wing test box by conducting structural static testing for three critical loading gives the sufficient confidence to the designers to go ahead with the implementing the same fabrication method for large structure like composite wing.

4. Geometry of wing test box

The wing test box was designed in two parts of which one section extends from station 6 to 10 having an approximate length of 1400 mm and the second section extends from station 4 to 6 having approximate length of 651 mm. The total span of wing test box is 2051 mm as shown in Fig. 4 (thick lines). The width of wing test box was 1277 mm constant along the length and the depth was 275 mm. Schematic diagram of wing test box is shown in same Fig. 4 when overlapped with similar region of the wing structure. The cross section of wing and wing test box where skins are spliced at station 6 is shown in Fig. 5 (dotted lines represents wing test box). It can be observed that the height of wing test box is more than wing structure at the spar locations where as the height of wing is more than wing test box in the centre region of the aerofoil.

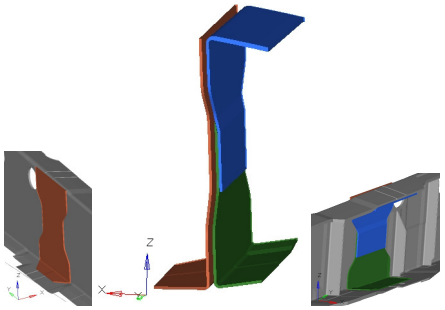

Fig. 3 Rear spar splice plates and front and rear views

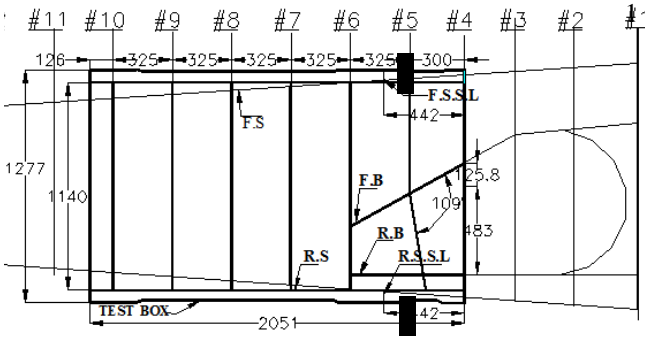

Fig. 4 Portion of wing considered for design of wing test box (Black spot on front and rear spars indicates the location of splicing where inboard and board spars are joined together

5. Layup sequence of composite components

The thickness and stacking sequence of top skin, bottom skin, front spar, rear spar and inter spar ribs in wing test box were kept the same as in the wing structure [3]. The thickness and stacking sequence of composite skins and ribs were locally modified as to make the structure suitable to receive heavy concentrated loads at selected locations of wing test box.

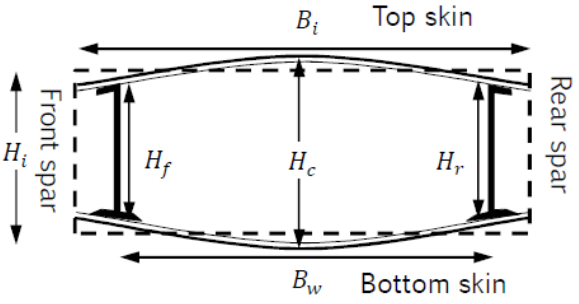

Fig. 5 Cross section of wing and wing test box

6. Material

The following materials were used for designing the wing test box. Resin system: EPOLAM 2063 manufactured by Ms. Axson Ltd. Reinforcement: HS CARBON UD FABRIC G0827-BB1040-HP03-1F manufactured by Ms. Hexcel Composites. The attachment fittings, where wing test box is mounted on to test rig, the points where shear force and bending moment applied as a concentrated load, are made up of mild steel.

7. Design philosophy of wing test box

At the first instance, it was assumed that the section is homogeneous and isotropic. Shear flow due to vertical shear force and bending stress level at various station of the wing test box were determined using principles of structural mechanics. The stress levels in skin, spar and other components were determined using classical lamination theory for critical loads and failure indices at ply levels were calculated. The first failure loads are used for sizing of wing test box at initial stage of design.

8. System of loading applied on wing test box

The main part of this paper is concentrated in arriving at a system of loading that should act on wing test box, which will induce the same shear stress flow level in spars splice plates as in the wing. The methodology and procedure adopted in arriving at one of such system of loading has been described in detail in the following section.

8.1. Shear force in wing

The shear flow distribution in a box structure is calculated based on the standard solution [4]. Consider the closed section beam of rectangular cross section shown in Fig. 6. Shear force S_x, S_y are applied through any point in the cross section and in generally cause direct bending stress and shear flow which are related by the equilibrium equation. It has been assumed that hoop stresses and body forces are absent, refer eq. (1).

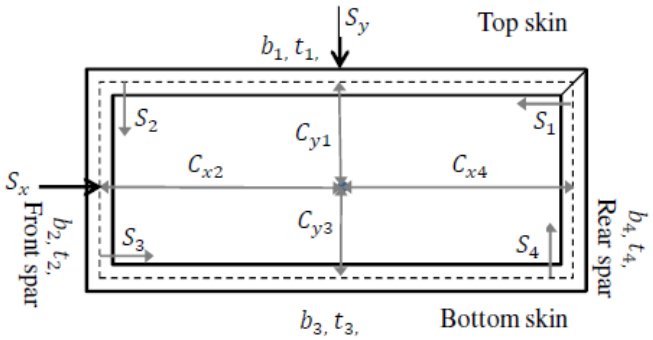

Fig. 6. Airfoil idealized into an equivalent rectangular box

$$\frac{\partial q}{\partial s} + t\frac{\partial \sigma_z}{\partial z} = 0 \quad \text{Eq. (1),}$$

Let $A_1 = -\left[\frac{S_x I_{xx} - S_y I_{xy}}{I_{xx} I_{yy} - I_{xy}^2}\right], A_2 = -\left[\frac{S_y I_{yy} - S_x I_{xy}}{I_{xx} I_{yy} - I_{xy}^2}\right]$ Eq. (2)

Now shear flow in any member is written in a simple form as given in eq. (3)

$$q_s = A_1 \int_0^s t.x.ds + A_2 \int_0^s t.y.ds \quad \text{Eq. (3)}$$

Shear flow in member top skin (1-2)

At $S_1 = 0$, $q_{b(1-2),0} = 0$; At $S_1 = b_1$, $q_{b(1-2),b_1} = A_1 t_1 \left[C_{x4}.b_1 - \frac{b_1^2}{2}\right] + A_2 t_1.[C_{y1}.b_1]$ Eq. (4)

Shear flow in member front spar (2-3)

At $S_2 = 0$, $q_{b(2-3)} = q_{b(1-2),b_1}$; At $S_2 = b_2$, $q_{b(2-3),b_2} = A_1 t_2.[C_{x2}.b_2] + A_2 t_2.\left[C_{y1}.b_2 - \frac{b_2^2}{2}\right] + q_{b(1-2),b_1}$ Eq. (5)

Shear flow in member bottom skin (3-4)

At $S_3 = 0$, $q_{b(3-4)} = q_{b(2-3),b_2}$; At $S_3 = b_3$, $q_{b(3-4),b_3} = A_1 t_3 \left[C_{x2}.b_3 + \frac{b_3^2}{2}\right] + A_2 t_3.[C_{y3}.b_3] + q_{b(2-3),b_2}$ Eq. (6)

Shear flow in member rear spar (4-1)

At $S_4 = 0$, $q_{b(4-1)} = q_{b(3-4),b_3}$; At $S_4 = b_4$, $q_{b(4-1),b_4} = A_1 t_4.[C_{x4}.b_4] + A_2 t_4.\left[C_{y3}.b_4 + \frac{b_4^2}{2}\right] + q_{b(3-4),b_3}$ Eq. (7)

8.2. Determination of shear force in each member

Shear force, F_i in individual members is determined by integrating shear flow q_i in that member w. r. t 'ds_i' ranging from '0 to b_i' for all members top and bottom skins and front and rear spars given in eq.(8).

$$A_1t_1\left[C_{x4}.\frac{b_1^2}{2}-\frac{b_1^3}{6}\right]+A_2t_1.\left[C_{y1}.\frac{b_1^2}{2}\right];\quad A_1t_2.\left[C_{x2}.\frac{b_2^2}{2}\right]+A_2t_2.\left[C_{y1}.\frac{b_2^2}{2}-\frac{b_2^3}{6}\right]+q_{b(1-2),b_1}.[b_2];\qquad \text{-Eq. (8a)}$$

$$A_1t_3\left[C_{x2}.\frac{b_3^2}{2}+\frac{b_3^3}{6}\right]+A_2t_3.\left[C_{y3}.\frac{b_3^2}{2}\right]+q_{b(2-3),b_2}.[b_3];\ A_1t_4.\left[C_{x4}.\frac{b_4^2}{2}\right]+A_2t_4.\left[C_{y3}.\frac{b_4^2}{2}+\frac{b_4^3}{6}\right]+q_{b(3-4),b_3}[b_4]\qquad \text{-Eq. (8b)}$$

8.3. Calculation of indeterminate shear flow

Take moment of shear force acting in individual members of open rectangular box determined in above eq. (8a) & (8b), about a corner where bottom skin and front spar is meeting.

$$F_{b(1-2)}.[C_{y1}+C_{y3}]-F_{b(4-1)}.[C_{x2}+C_{x4}]+2Aq_{(0)}=0,\ \text{Eq. (9)};\quad q_{(0)}=(-)\frac{F_{b(1-2)}.[C_{y1}+C_{y3}]-F_{b(4-1)}.[C_{x2}+C_{x4}]}{2A}\qquad \text{Eq. (10)}$$

8.4. Solution for shear center of a closed rectangular section

Let, 'e_x' be the position of shear center measured from the centerline of front spar, S_y is the shear load, if acts through the shear center of a section produce zero twist. Transforming open rectangular section in to closed rectangular section given by eq-(11).

$$q_0\left[\frac{b_1}{t_1}+\frac{b_2}{t_2}+\frac{b_3}{t_3}+\frac{b_4}{t_4}\right]-\frac{e_x.S_y}{2A}\left[\frac{b_1}{t_1}+\frac{b_2}{t_2}+\frac{b_3}{t_3}+\frac{b_4}{t_4}\right]=\left[\frac{F_{(1-2)}}{t_1}+\frac{F_{(2-3)}}{t_2}+\frac{F_{(3-4)}}{t_3}+\frac{F_{(4-1)}}{t_4}\right]\qquad \text{Eq. (11)}$$

Solve above equation for 'e_x'.

9. Idealization of wing (airfoil) into an equivalent rectangular box

The main sectional properties of wing structure that govern the shear flow around airfoil shape are moment of inertia terms (I_{xx}, I_{yy}, I_{xy}) and 'A' area enclosed by all center lines of top, bottom skins and web of front and rear spars. The cross section of actual wing structure and idealized equivalent rectangular section are shown in Fig.7. The sectional properties of idealized rectangular section should be of more or less equal to that of sectional properties of actual wing section (airofoil). To have sectional properties of idealized rectangular section similar to that of actual wing sections, the following points were considered.

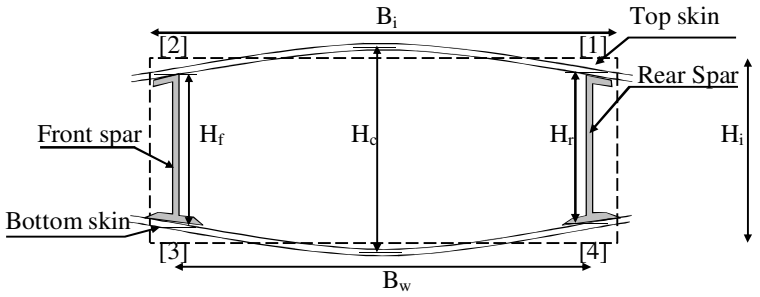

Fig.7. Cross section of wing structure (airfoil shape), and idealized wing structures into an equivalent rectangular section (dotted line).

i. Adjustment of the width of idealized rectangular section so that B_i can be more than width of actual wing structure (B_w).

ii. The depth of idealized rectangular section cannot be less than minimum height of actual wing section at spar locations and cannot be more than maximum height of wing section at center region of airfoil.

Shear flow around idealized rectangular section can be determined using well-established methods. It is obvious that shear flow in such idealized section is not replica of expected shear flow in actual wing structure. An approximation to this effect was made so as to transform the shear flow from one section to the other section proportionate to the height ratio as given in the following section.

10. Conversion of shear flow from idealized section to the wing section

After determining the shear flow distribution for idealized section, an approximate shear flow distribution in actual wing section is obtained by equating total shear force in their respective spars of actual wing to wing test box as given as follows. The numerical subscription of

shear flow indicates the number of point shown in Fig. 7 and superscription of shear flow indicates 'w' for wing and 'i' for idealized sections and so on for other terms. Let, B_w, B_i, be the width of actual wing section and idealized rectangular section respectively. H_f^w, Height of front spar of actual wing section, H_r^w, Height of rear spar of actual wing section, H_c^w, Max height of wing of actual wing section, H_i, Height of front spar, q_n^i, Shear flow in **i**dealized section at **n**th point, q_n^w Shear flow in actual **w**ing section at **n**th point, *(1),* Junction of top skin and rear spar, *(2)*, Junction of top skin and front spar, *(3)*, Junction of bottom skin and front spar, *(4)*, Junction of bottom skin and rear spar. The shear flow in wing structure is given at node 1 to 4 mentioned in Fig. 7 are given in eq. (12).

$$q_1^w = q_1^i\left[\frac{H_r^i}{H_r^w}\right] \quad , \quad q_2^w = q_2^i\left[\frac{H_f^i}{H_f^w}\right], \quad q_3^w = q_3^i\left[\frac{H_f^i}{H_f^w}\right] \quad , \quad q_4^w = q_4^i\left[\frac{H_r^i}{H_r^w}\right] \qquad \text{Eq. (12)}$$

10.1. Transformation of shear flow from wing to the wing test box

After determining shear flow in actual wing structure as explained above from eq. (12), the numerical values of shear flow were imported to the wing test box. This ensures that point 1 to 4 of wing test box would also see the same shear stress flow level as in the actual wing section. As geometry of wing differed from that of wing test box, the shear force that should act in wing test box to have same shear stress will be different from that shear force acting in actual wing structure. The shear force acting on wing test box was determined as given in below eq. (13). Overall dimension of idealized wing section and wing test box schematically represented in Fig. 8. It is seen that the dimensions of wing test box is more than that of idealized wing section. Therefore, the sectional properties are different one from the other. The mathematical condition that governs to have same shear flow values in wing test box and actual wing section are given in the following eq. (13) and represented in Fig. 9.

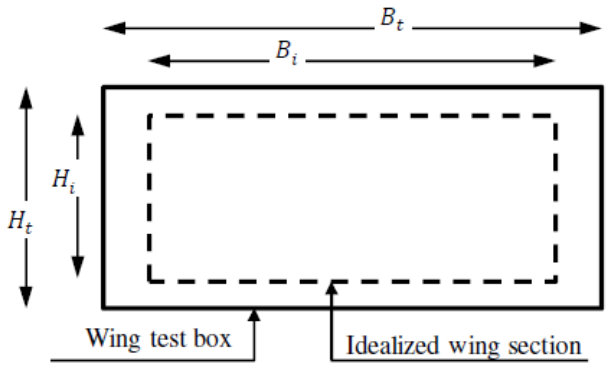

Fig.8. Line diagram of wing test box and idealized wing section (dotted line

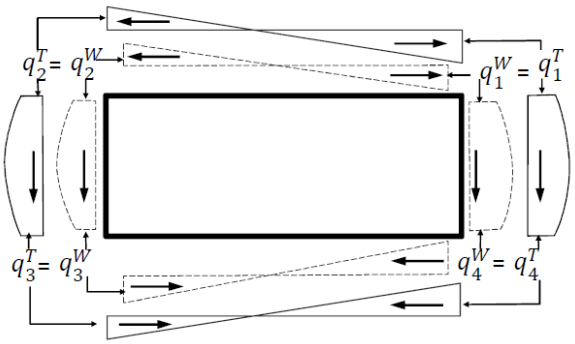

Fig.9. Shear flow distribution around wing section (dotted) and WTB (firm line)

$$q_1^T = q_1^w \; ; \; q_2^T = q_2^w \; ; \; q_3^T = q_3^w \; ; \; q_4^T = q_4^w \; ; \; q_f^T = q_f^w \; ; \; q_r^T = q_r^w \qquad \text{Eq. (13)}$$

10.2. An example of transforming shear flow from wing to wing test box

The geometrical details and stacking sequence of all composite parts under consideration were substituted in all above mathematical equations. The critical load case was selected for determining the shear flow for transformation from wing to wing test box. Shear flow distribution from an idealized wing section, actual wing section, and that shear flow to be applied on wing test box, actual shear flow distribution applied on wing test box are shown in Fig.10 to Fig. 13 respectively.

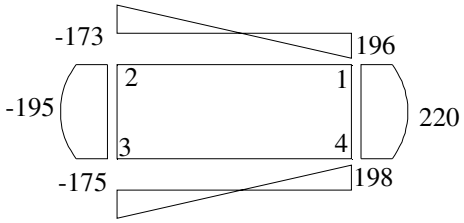

Fig. 10 Shear flow distribution in an idealized section at station #6 for V_d case (DUL)

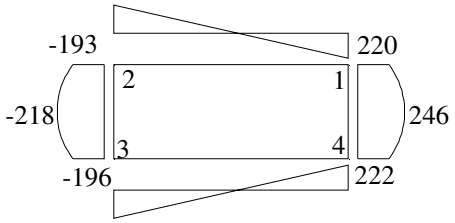

Fig. 11 Shear flow distribution in actual wing section at station #6-V_d case (DUL)

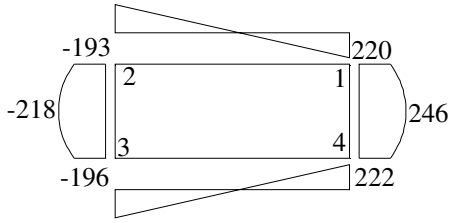

Fig. 12 Shear flow distribution to be applied in wing test box at station #6 –V_d case (DUL)

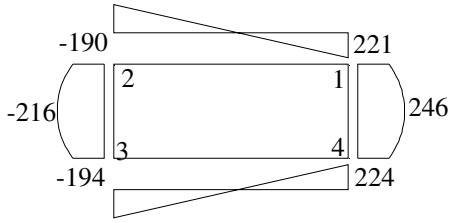

*Fig. 13 Shear flow distribution found in the wing test box at station #6 –V_d case (DUL) when shear force of **121094** N applied at an eccentricity of **70 mm** from shear center of wing test box*

11. A new system of loading acting on wing test box

The system of loading to be applied on wing test box for a critical load case was worked based on shear flow calculation shown above. The values of point load needs to be applied on front spar, rear spar at each station of wing test box is shown in Table 1. The shear force acting on wing test box and actual wing structure for a given case is shown in Fig. 14, which shows that the shear force values at spar splicing region is exactly matching with the aerodynamic load distribution on wing structure. However this position of point of application load is different as to simulate the torsion effect. The application of shear force on wing test box during testing is shown in Fig. 15.

Table 1 Load to be applied on wing test box for Vd case at design ultimate load

Station	#4	#5	#6	#7	#8	#9	#10
X-Coordinate, m	0.95	1.25	1.575	1.91	2.225	2.55	2.875
Load on Front Spar, N	-	-	-	7876	21292	22619	-
Load on Rear Spar, N	-	-	-	10540	28493	30271	-
Position of center of loading system from the center line of front spar towards rear spar, m	-	-	-	0.641	0.641	0.641	-

12. Conclusion

The shear flow distribution around a closed rectangular cross section unsymmetrical about both axes, subjected to biaxial shear loading, and torque is presented. It also explained an approximate procedure adopted for transforming the shear stress flow from airfoil of wing structure to a regular closed rectangular cross section, which has ultimately been used in arriving at a system of loading that should be applied on wing test box. Such system of loading induced shear stress flow level in the spar splice joint of wing test box same as actual wing structure. The system of loading worked by the methodology was applied on front and rear spars at appropriate locations along the spar of wing test box using hydraulic jacks. The wing test box withstood design ultimate load successfully without any defects noticed in the spar splice plates.

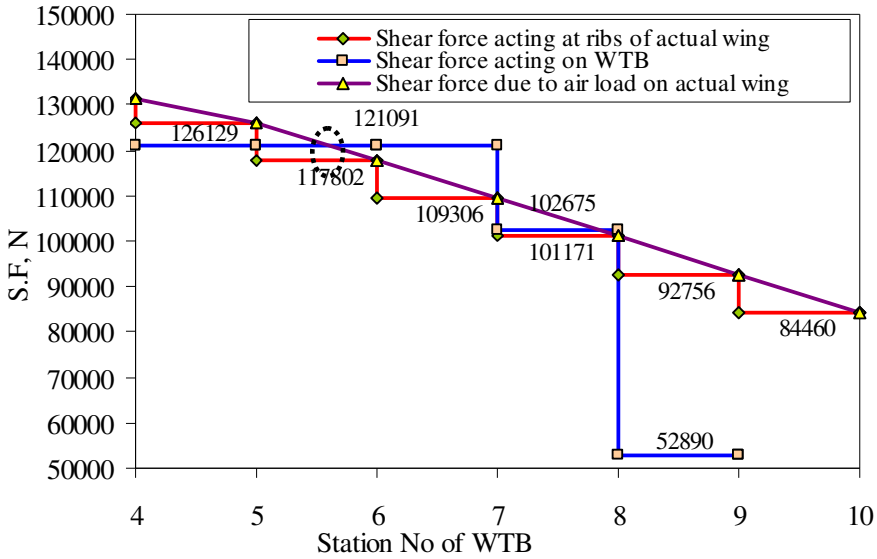

Fig.14. System of loading worked out to apply on wing test box. Encircled point is the place where the shear force on wing structure and wing test box is simulated.

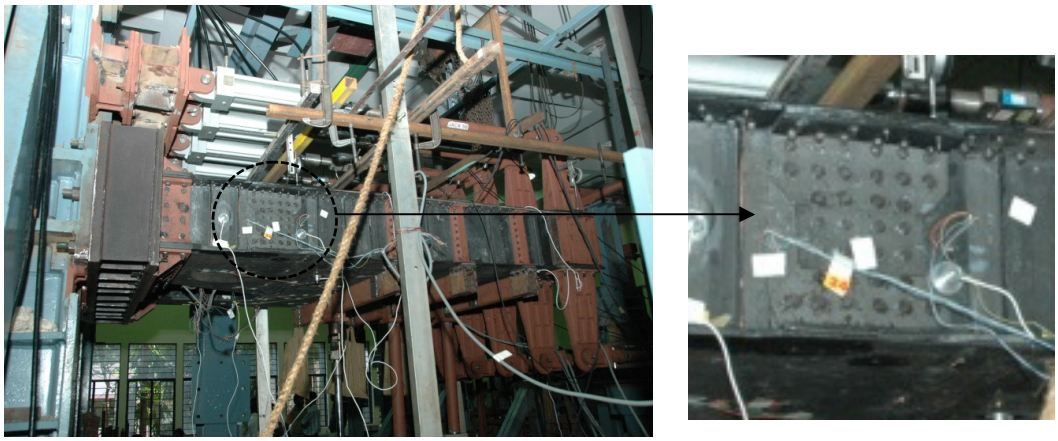

Fig.15. Wing test box mounted on test rig System of loading applied on wing test box though hydraulic jacks and splice plates where shear flow is simulated during testing on wing test box

Acknowledgement

Authors thank Shri. Shyam Chetty, Director of CSIR-National Aerospace Laboratories, and Shri. H. N Sudheendra, Head and Dr. Ramesh Sundaram, Deputy Head, Advanced Composites Division for extending the technical, administrative and financial support for completing this work.

Reference

1. Polagangu James and Gaddikeri Kotresh, Byji Varughese (2008) "Design of spar slice joints in composite wing structures", Proceedings of the International Conference on Aerospace Science and Technology (INCAST 2008-044), 26-28 Jun 2008, Bangalore.

2.Murali Krishna, D and Ramanaiah, B, Polagangu James, Kotresh M. Gaddikeri, Varughese, Byji and Subba Rao, M (2007) "Experimental investigation on a mechanically fastened splice joint in a composites aircraft wing", 15th National Conference on Aerospace Structures, 15-16 Oct 2007, Coimbatore, Tamil Nadu, India.

3. Gaddikeri Kotresh, Polagangu James, Byji Varughese, M. Subba Rao, et al., "Design of Composite Wing for SARAS Aircraft", PD-AC- 0714, November, 2007, Advanced Composites Division, CSIR-National Aerospace Laboratories, Bangalore, India.

4. T. H. G. Megson, Airframe structures for Engineering Students", Second Edition, 1990, Edward Arnold.